



Article

Anti-Inflammatory Effects of SGLT1 Synthetic Ligand in In Vitro and In Vivo Models of Lung Diseases

Cristiano Rumio ^{1,*}, Giuseppina Dusio ¹, Diego Cardani ¹, Barbara La Ferla ²  and Giuseppe D'Orazio ^{3,*} 

¹ Department of Pharmacological and Biomolecular Sciences, Università degli Studi di Milano, Via Balzaretti 9, 20133 Milan, Italy

² Department of Earth and Environmental Sciences DISAT, Università degli Studi di Milano-Bicocca, Piazza della Scienza 1, 20126 Milan, Italy; barbara.laferla@unimib.it

³ Department of Chemistry, Università degli Studi di Milano, Via C. Golgi 19, 20133 Milan, Italy

* Correspondence: cristiano.rumio@unimi.it (C.R.); giuseppe.dorazio@unimi.it (G.D.)

Abstract: Background. Several research findings suggest that sodium–glucose co-transporter 1 (SGLT1) is implicated in the progression and control of infections and inflammation processes at the pulmonary level. Moreover, our previous works indicate an engagement of SGLT1 in inhibiting the inflammatory response induced in intestinal epithelial cells by TLR agonists. In this study, we report the anti-inflammatory effects observed in the lung upon engagement of the transporter, and upon the use of glucose and BLF501, a synthetic SGLT1 ligand, for the treatment of animal models of lung inflammation, including a model of allergic asthma. **Methods.** In vitro experiments were carried out on human pneumocytes stimulated with LPS from *Pseudomonas aeruginosa* and co-treated with glucose or BLF501, and the production of IL-8 was determined. The anti-inflammatory effect associated with SGLT1 engagement was then assessed in in vivo models of LPS-induced lung injury, as well as in a murine model of ovalbumin (OVA)-induced asthma, treating mice with aerosolized LPS and the synthetic ligand. After the treatments, lung samples were collected and analyzed for morphological alterations by histological examination and immunohistochemical analysis; serum and BALF samples were collected for the determination of several pro- and anti-inflammatory markers. **Results.** In vitro experiments on human pneumocytes treated with LPS showed significant inhibition of IL-8 production. The results of two in vivo experimental models, mice exposed to aerosolized LPS and OVA-induced asthma, revealed that the engagement of glucose transport protein 1 (SGLT1) induced a significant anti-inflammatory effect in the lungs. In the first model, the acute respiratory distress induced in mice was abrogated by co-treatment with the ligand, with almost complete recovery of the lung morphology and physiology. Similar results were observed in the OVA-induced model of allergic asthma, both with aerosolized and oral BLF501, suggesting an engagement of SGLT1 expressed both in intestinal and alveolar cells. **Conclusions.** Our results confirmed the engagement of SGLT1 in lung inflammation processes and suggested that BLF501, a non-metabolizable synthetic ligand of the co-transporter, might represent a drug candidate for therapeutic intervention against lung inflammation states.

Keywords: sodium–glucose co-transporter 1 (SGLT1); lung inflammation diseases; ovalbumin (OVA)-induced asthma; glycoderivatives



Citation: Rumio, C.; Dusio, G.; Cardani, D.; La Ferla, B.; D'Orazio, G. Anti-Inflammatory Effects of SGLT1 Synthetic Ligand in In Vitro and In Vivo Models of Lung Diseases. *Immuno* **2024**, *4*, 502–520. <https://doi.org/10.3390/immuno4040031>

Academic Editor: Bashar Saad

Received: 18 September 2024

Revised: 9 October 2024

Accepted: 6 November 2024

Published: 8 November 2024



Copyright: © 2024 by the authors. Licensee MDPI, Basel, Switzerland. This article is an open access article distributed under the terms and conditions of the Creative Commons Attribution (CC BY) license (<https://creativecommons.org/licenses/by/4.0/>).

1. Introduction

Acute pneumonic processes and diseases are physiopathological states that have risen to prominence during the last few years due to the COVID-19 world outbreak and emergency. The disease could lead a minor percentage of infected people to severe illness, characterized in particular by extensive damage at the pulmonary level and subsequent hypoxemic respiratory failure [1]. Severe forms of illness are also characterized by subsequent progression to ARDS (acute respiratory distress syndrome), in which aggressive

inflammatory responses occur [2]. The uncontrolled inflammation response, caused by a massive release of pro-inflammatory cytokines (cytokine storm) [3] in response to viral and/or secondary infections (or due to a dysregulated host response), can ultimately lead to a systemic acute inflammation state, characterized by multi-organ damage and failure, in particular on cardiac, kidney, and hepatic levels [4].

The lung epithelium, similar to the intestinal epithelium, acts as a physical barrier between the host and the environment, offering passive protection against harmful agents. Additionally, the lung epithelium can trigger active responses, including mechanical clearance, the production of antimicrobial substances, and involvement in the development of adaptive immune responses. Responses against infectious agents include acute inflammatory reactions with local recruitment and activation of polymorphonuclear leukocytes [5], and the release of pro-inflammatory molecules [6,7], proteases, reactive oxygen species, and nitrogen species [8,9]. These processes may cause undesired alveolar–capillary damage with high-permeability pulmonary edema [10]. These inflammatory responses are the consequence of the ability of lung epithelial cells, also called pneumocytes, to recognize microorganisms through pattern recognition receptors. Like many other epithelia, the lung epithelium expresses Toll-like receptors (TLRs) [11,12], which play a key role in the recognition of microorganisms and the subsequent induction of both innate and adaptive immune responses, directly or via the production of inflammatory mediators like cytokines and chemokines, and antimicrobial peptides.

In previous work, we have reported [13] that the inflammatory response induced in intestinal epithelial cells by TLR agonists is inhibited by glucose upon engagement of the sodium–glucose transporter SGLT1 [14]. Similarly to intestinal epithelial cells, pneumocytes have been reported to also express SGLT1 [15–17]; this led us to ask whether the engagement of SGLT1 could inhibit inflammatory damage to the lungs by TLR agonists, as we had observed this phenomenon in inflammatory damage to the intestinal mucosa. Any positive result in this setting would suggest the possibility of a novel approach to the treatment of inflammatory lung diseases. Moreover, recently, a significant role for SGLT1 in the progression and control of pulmonary infection and inflammation processes has been established. In particular, research works suggest that enhanced SGLT1 activity and, on the contrary, its loss of function are associated with the prevention of bacterial proliferation and increased lung tissue inflammation, respectively [18–20]. We observed in our previous work [13] that high amounts of orally administered glucose were necessary to induce anti-inflammatory effects, amounts unlikely to be useful in repeat-treatment protocols. Therefore, we screened a library of glucose derivatives for their ability to engage SGLT1 and induce anti-inflammatory effects at lower concentrations than that of glucose; these activities led to the identification of a non-metabolizable, synthetic SGLT1 ligand, named BLF501 (Figure 1), which induced anti-inflammatory effects *in vivo* at concentrations five orders of magnitude lower than glucose itself [21]. BLF501 is a C-glucoside, a type of carbohydrate derivative in which a carbon atom substitutes the anomeric oxygen. This substitution significantly enhances the chemical and metabolic stability of this class of compounds [22]. Glycoderivatives and glycomimetics, which are derived from carbohydrates, have garnered increasing interest in drug development. They hold promise as potential drug candidates, including anti-diabetic, antiviral, and antitumor compounds [23–34]. Their significance in drug discovery stems from their ability to overcome the limitations of natural carbohydrates, such as low stability under physiological conditions and poor drug-like properties. Our research has demonstrated a significant protective role of BLF501 in the intestinal mucosa during chemotherapy-induced mucositis [35]. Additionally, we have recently developed a set of gold nanoparticles (AuNPs) decorated with derivatives of D-glucose and BLF501 [36]. These AuNPs can be used as chemical tools to assess the multivalent activation of SGLT1, as supported by the existing literature [37–40]. In this article, we report on the anti-inflammatory effects that are observed in the lungs upon engagement of SGLT1 and upon the use of BLF501 for the treatment of animal models of inflammatory lung diseases, including a model of allergic asthma [41].

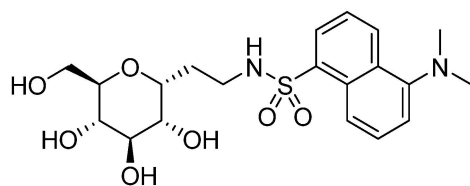


Figure 1. Structure of BLF501, synthetic ligand of SGLT1.

2. Materials and Methods

2.1. Cells and Cell Treatments

Human lung carcinoma epithelial cells (A549), derived from type II pneumocytes, human enterocyte cells (HT29), and human bronchial epithelial cells (16-HBE) were obtained from the American Type Culture Collection (Manassas, VA, USA). The cells were maintained in Dulbecco's modified Eagle's medium (Sigma-Aldrich, Saint Louis, MO, USA) supplemented with 10% fetal bovine serum (FBS, Gibco, Invitrogen Corp., Auckland, New Zealand), 200 U/mL penicillin, and 200 µg/mL streptomycin (Sigma-Aldrich) (complete medium). Cells were grown at 37 °C in a humidified atmosphere with 5% CO₂. Human monocytic leukemia cells THP-1 were maintained in RPMI-1640 medium (Sigma-Aldrich) supplemented with 10% FBS, 200 U/mL penicillin, and 200 µg/mL streptomycin.

For treatments, A549, 16-HBE, and HT29 cells were cultured for 18 h in complete medium, in complete medium supplemented with a high D-glucose concentration (5 g/L) (Merck, Darmstadt, Germany), or in medium containing BLF501 (50 µg/L) before stimulation with LPS from *Pseudomonas aeruginosa* (100 µg/mL) (Sigma-Aldrich) for 6 h. Supernatants were collected at the end of treatment and stored at −80 °C. In some experiments with HT29 cells, TNF-α (Peprotech Inc., Rocky Hill, NJ, USA) was added at 50 ng/mL for 6 h at the end of the 18 h culture period.

2.2. Co-Culture of HT29 and Dendritic Cells

Human PBMCs were isolated by Ficoll–Paque density gradient centrifugation of buffy coats obtained from healthy volunteers (INT, Milan, Italy). CD14⁺ monocytes were positively selected using anti-CD14⁺ microbeads. Monocytes were induced to differentiate to immature MoDCs in 5- to 6-day culture in RPMI 1640 complete medium supplemented with 50 ng/mL GM-CSF and 50 ng/mL IL-4. The purity of monocytes and MoDCs, routinely checked by flow cytometric analysis, was more than 90%. The following antibodies were used: anti-CD14-FITC (M5E2) and anti-CD1a-FITC (HI149). All of the antibodies were purchased from BD Bioscience Pharmingen, San Diego, CA, USA. MoDCs cells (1×10^5) were cultured in multi-well supports; the day after, HT29 cells were seeded at 1×10^6 cells/well in the upper part of a Transwell growth support (Millipore, Billerica, MA, USA), which was put in the same wells containing MoDCs. When HT29 cells reached confluence, they were incubated for 18 h with BLF501 and then stimulated for 6 h with LPS as previously described. Untreated cells or cells treated with BLF501 alone or LPS alone served as controls. At the end of these incubations, supernatants were collected.

2.3. Small Interfering RNA (siRNA)

The expression of SGLT1 was silenced by transfection with siRNA. Briefly, cells (2×10^5 /well) seeded in 6-well plates at 60–80% confluence were washed in Optimem medium (Invitrogen Corp.) and then transfected with a pool of siRNA oligonucleotides targeting human SGLT1 mRNA or a scrambled RNA duplex (Santa Cruz Biotechnology Inc., Santa Cruz, CA, USA) at a final concentration of 100 nM. Then, 6 µg/µL Lipofectamine 2000 (Invitrogen Corp.) was used as a transfection reagent. After 24 h, the transfection mixture was aspirated from the cells, replaced with culture medium, and incubated for 24 h with BLF501 or glucose in the presence of LPS or TNF-α, as reported above. For transfection and knockdown gene efficacy analysis, the cells were lysed and analyzed with a qPCR protocol.

2.4. Enzyme-Linked Immunosorbent Assay (ELISA)

Quantification of KC, NO, IgE, IL-4, IL-5, IL-8, IL-10, IL-12, TNF- α , and IFN- γ in serum samples or culture supernatants was performed using commercially available ELISA kits (Quantikine, R&D Systems, Minneapolis, MN, USA; Promega Corporation, Madison, WI, USA; MD Biosciences, Zürich, Switzerland; Endogen, Woburn, MA, USA; BD Biosciences, San Diego, CA, USA), according to the manufacturers' instructions. The enzymatic reaction was detected in an automatic microplate photometer (Multiskan Ascent, Thermo Electron Corporation; Vantaa, Finland).

For the quantification of hsp27 and its murine homolog hsp25, 96-well plates (NUNC Thermo Fisher Scientific Inc., Rochester, NY, USA) were coated with 10 μ L/well of cell supernatant and left overnight at 4 °C. After three washes with PBS and 0.5% Tween 20, the plates were incubated for 60 min at room temperature with a primary rabbit anti-hsp27 antibody (Novus Biologicals, Littleton, CO, USA), diluted at 1:2000 in Assay diluent (PBS, 0.5% Tween 20, 5% FBS, 100 μ L/well). After three washes, the plates were incubated for 60 min at room temperature with a secondary biotinylated anti-rabbit antibody (Vector Laboratories, Burlingame, CA, USA) diluted at 1:1000 in Assay diluent (100 μ L/well). After three washes, streptavidin-conjugated horseradish peroxidase (SA-HRP, 1:250 in Assay diluent, 100 μ L/well) was added to the plates for 30 min. After seven further washes, 100 μ L of tetramethylbenzidine (TMB) substrate (0.1 mg/mL 0.05 M phosphate-citrate buffer, pH 5.0) was added to each well and incubated at RT. The reaction was stopped within 50 min with 20 μ L of 2M H₂SO₄ and read at 450 nm (absorbance filter) using an automatic microplate photometer.

2.5. Exposure of Mice to Aerosolized LPS

Male C57BL/6 mice were purchased from Charles River (Calco, Italy). They were maintained under specific pathogen-free conditions. The experimental protocols were approved by the Ethics Committee for Animal Experimentation of the Istituto Nazionale dei Tumori (INT) (Milan, Italy) according to UKCCCR guidelines. The animals were exposed to aerosolized LPS from *Pseudomonas aeruginosa* in a whole-animal exposure system. For this purpose, the animals were placed in wire mesh cages within a 55-l Plexiglas cylinder connected via 10 cm ducting to a 16 l aerosol chamber. Airflow through the system was maintained at 20 l/min by negative pressure. Aerosols were generated from twin jet nebulizers (Salter Labs, Arvin, CA, USA), each containing 3 mL of LPS suspension (3 mg/mL) and driven by forced air at 15–18 psi. After 30 min, the chamber was purged with ambient air, and the mice were returned to their microisolator cages. Some of the mice were also concomitantly exposed to aerosolized BLF501 (266 ng/mL, for a total of 3 mL). These treatments were carried out for five consecutive days. In another experiment, mice were treated p.o. with BLF501 before exposure to aerosolized LPS.

2.6. Asthma Model

Male C57BL/6 mice were immunized i.p. with 100 μ g of ovalbumin (OVA grade V; Sigma-Aldrich) and 500 μ g of aluminum hydroxide (Alum, Sigma-Aldrich). Concomitantly, a second group of animals was treated with 25 μ g/Kg of BLF501 by oral and/or aerosolized administration. One week after the first immunization, the same treatments were repeated. Two weeks after the first immunization, the first group of animals was challenged for 25 min with aerosol administration of 5% (wt/vol) OVA in PBS each day, for 5 consecutive days, while the second group received OVA plus oral (25 μ g/Kg) and/or aerosolized (266 ng/mL, for a total of 3 mL) BLF501. To investigate the involvement of TNF- α in the asthmatic process, a group of animals was also administered a neutralizing anti-TNF- α antibody (R & D System, Minneapolis, MN, USA) at 15 μ g/mouse, i.p., during the 4th and 5th day of OVA plus BLF501 administration. Two hours after the last inhalation, blood samples were collected from the orbital artery, mice were sacrificed, and BALF sampling was performed.

2.7. Broncho-Alveolar Lavage

Broncho-alveolar lavage was performed by instilling 1 mL saline into the lungs through a tracheal cannula three times and then gently aspirating the fluid. The recovered fluid was filtered through a double layer of gauze to remove mucus. The resulting broncho-alveolar lavage fluid (BALF) was centrifuged (1000 rpm, 4 °C, 10 min), supernatants were collected and stored at –80 °C, while cells were fixed in formalin with the addition of sucrose (VWR International, Poole, England). Total BALF cell counts were performed, and aliquots were pelleted on glass slides by cytocentrifugation (Shandon Inc., Pittsburgh, PA, USA). Differential counts were performed on Giemsa (Fluka, St. Gallen, Switzerland)-stained cytopins.

2.8. Hematoxylin–Eosin Staining

Lungs collected from animals were fixed by inflation with 10% paraformaldehyde and embedded in paraffin. Sections were cut at 4 µm thickness, deparaffinized, rehydrated, stained with hematoxylin and eosin, and mounted in Entellan® (Merck). Slides were observed under a Nikon Eclipse 80i microscope equipped with a digital Nikon DS-L1 camera (Nikon Instruments, Firenze, Italy).

2.9. Immunohistochemistry

The expression of ICAM-1, caveolin-1, and NF-κB in lung samples was assessed immunohistochemically. In brief, 4 µm sections of paraffin-embedded samples were deparaffinized and endogenous peroxidases were quenched for 20 min with 0.3% (*v/v*) hydrogen peroxide in PBS. The sections were incubated with goat anti-mouse ICAM-1 (1:10 in PBS, R&D Systems) or rabbit anti-mouse caveolin-1 (1:200 in PBS, Santa Cruz Biotechnology Inc.) polyclonal antibodies. For NF-κB, a mouse antibody for murine NF-κB p65 (sc-8008, Santa Cruz B.) and the M.O.M. Immunodetection Kit (Vector Laboratories) were used. Sections were washed with PBS and incubated with secondary antibodies at room temperature (RT). Specific labeling was detected with a DAB Substrate Kit for peroxidase (Vector Laboratories).

2.10. Immunofluorescence

For immunofluorescence experiments, antigen retrieval was carried out and murine sections of the lung were incubated with 0.1 M glycine buffer for 20 min at RT and then with sodium tetrahydroborate solution for 20 min at RT. For the immunofluorescence analysis of the expression of SGLT1 on pneumocytes, the polyclonal anti-SGLT-1 antibody (Millipore) was used, diluted at 1:1000 in PBS, for 1 h at room temperature. For dendritic cell staining, slices were incubated with biotinylated anti-CD11c antibody (BD Biosciences) for 2 h at 37 °C, diluted at 1:50 in PBS and 3% bovine serum albumin (BSA, Sigma-Aldrich). Secondary detection was performed in both cases with a goat anti-rabbit antibody Alexa 488 (Invitrogen Corp.), diluted at 1:200 in PBS and 3% BSA for 30 min at RT. Nuclei were counterstained with 4,6-diamidino-2-phenylindole and the slides were mounted with Mowiol mounting medium.

2.11. Isolation of Murine Dendritic Cells

Lung tissue was placed in PBS, DTT (145 µg/mL), and EDTA (0.37 mg/mL), dissected (<2 mm in size), and digested with collagenase type 2 (Sigma Aldrich) at a final concentration of 10 mg/mL in RPMI and DNase (Bovine Pancreatic DNase, Sigma-Aldrich) at a final concentration of 25 mg/mL for 60 min at 37 °C under gentle shaking. After this enzymatic digestion, the lung samples were gently broken apart using a 2 mL syringe to produce a single-cell suspension and centrifuged at 1500 rpm for 5 min at 4 °C. The single-cell suspension was washed with PBS containing 0.5% FBS, and the cells were then counted and, following pre-incubation with an anti-Fc receptor antibody (Miltenyi Biotec S.r.l., Calderara di Reno, Italy), incubated at the appropriate ratio with MACS CD11c microbeads (Miltenyi Biotec S.r.l.) for 15 min at 4 °C. After being washed again with PBS containing

0.5% FBS, the cells were separated by passing the antibody-coated cell suspension over a VS+ column on a SuperMACS magnetic cell separator (all from Miltenyi Biotec S.r.l.). CD11c-positive cells were collected by removing the column from the magnetic field and then flushing it with PBS-0.5% FBS. Thereafter, the cells were washed with RPMI medium, counted, and plated in vitro for 18 h. At the end of this period, supernatants were harvested for the determination of cytokines.

2.12. Statistical Analysis

Student's *t*-test (paired two-tailed) and GraphPad Prism software version 10 (GraphPad Prism Software Inc., San Diego, CA, USA) were used for comparisons between groups. *p* values less than 0.05 were considered significant.

3. Results

3.1. The Engagement of SGLT1 Inhibits the Response of Human Pneumocytes to LPS

The screening of a library of synthetic glucose analogues allowed us to identify a synthetic SGLT1 ligand, named BLF501, which inhibits LPS-induced IL-8 production in intestinal epithelial HT-29 cells at 100,000-fold lower concentrations than D-glucose [21]. Consequently, we investigated whether d-glucose and its synthetic analogue BLF501 inhibit LPS-induced IL-8 production in A549 human pneumocytes which express SGLT1, according to data previously reported on rat pneumocyte type II cells [15]. For this purpose, cells were cultured for 18 h in the presence of a D-glucose concentration 5× higher than that of normal medium ("high-D-glucose" medium, 27.78 mM) or 500 µg/L of BLF501 (1.1 µM) and subsequently stimulated for 6 h with LPS from *Pseudomonas aeruginosa* (100 µg/mL). The BLF501 dosage was chosen following preliminary dose–response experiments (Supplementary Materials, Figure S1). The addition of D-glucose or BLF501 suppressed IL-8 production in LPS-stimulated A549 cells to levels similar to those of unstimulated cells (LPS 9190 ± 664 pg/mL; D-glucose/LPS 884 ± 64 pg/mL, $p = 1.94 \times 10^{-11}$ vs. LPS; BLF501/LPS 903 ± 42 pg/mL, $p = 2.40 \times 10^{-11}$ vs. LPS, Figure 2A). When the same experiments were performed on the human bronchial epithelial cell line 16-HBE, LPS-induced IL-8 production was not inhibited by D-glucose or BLF501 treatment (Figure 2B). D-glucose and BLF501 also inhibited other LPS-induced responses in A549 cells such as NO production (Supplementary Materials, Figure S2) [42,43]. The involvement of SGLT1 in glucose- or BLF501-induced inhibition of LPS-induced responses in A549 cells was confirmed by silencing SGLT1 expression with siRNA. Thus, upon the addition of SGLT1 mRNA-specific siRNA, the inhibitory effect of D-glucose and BLF501 on LPS-induced IL-8 production was abrogated (LPS 9115 ± 563 pg/mL; D-glucose/LPS 8973 ± 531 pg/mL; BLF501/LPS 9029 ± 311 pg/mL) (Figure 2A). These results highlight the essential role of SGLT1 in glucose- and BLF501-induced inhibition of LPS-driven inflammatory responses in human pneumocytes.

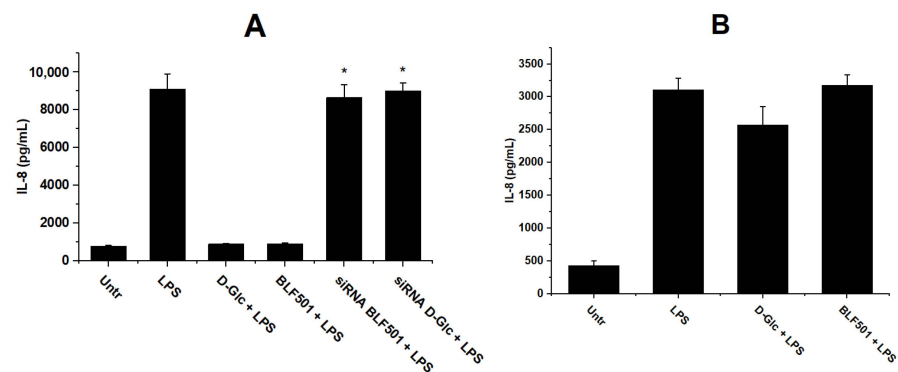


Figure 2. (A) IL-8 levels in culture medium of A549 after treatment with *P. aeruginosa* LPS and IL-8 level in culture medium of A549 cells upon SGLT1 silencing with mRNA-specific siRNA and LPS treatment. * $p = 6.25 \times 10^{-9}$ vs. BLF501 + LPS; * $p = 2.94 \times 10^{-10}$ vs. D-Glc + LPS. Knockdown efficiency of SGLT1 gene was more than 70% (by qPCR analysis). (B) IL-8 levels in culture medium of 16-HBE cells.

3.2. Anti-Inflammatory Effects Induced by Engagement of SGLT1 by BLF501 Protect Lungs from Injury Due to Aerosol Administration of LPS

The immunofluorescence analysis performed on normal lung samples confirmed that pneumocytes expressed SGLT1, while the bronchial epithelium was not stained (Supplementary Materials, Figure S3). We then assessed whether SGLT1 engagement exerted anti-inflammatory effects in an *in vivo* model of LPS-induced lung injury. Given that BLF501 was designed and synthesized to act as a d-glucose agonist on SGLT1 and the *in vitro* results confirmed this assumption, *in vivo* experiments were performed only with BLF501. The compound was administered via aerosol at a dose (25 µg/kg, corresponding to 266 ng/mL, for a total of 3 mL of administered solution) that had been chosen based on preliminary dose–response experiments. Groups of mice ($n = 10$) were treated via aerosol administration with a solution containing 3 mg/mL LPS (3 mL), with a solution of BLF501 (266 ng/mL, 3 mL), or concomitantly with both (same dosage, 3 mL totally). The treatments were administered daily for five consecutive days. At the end of this period, blood and lung samples were collected from all animals. As shown in Figure 3A, the lungs of mice exposed to LPS exhibited significant inflammatory changes. These changes included alveolar hemorrhage and extensive extravasation of both mono- and polymorphonuclear leukocytes into the alveolar spaces, forming clusters. Numerous eosinophils and neutrophils were also observed. Some neutrophils were present in the bronchial spaces, along with many macrophages. The bronchial epithelium showed extensive regressive changes, including local epithelial loss, areas of proliferation with rare superficial mitosis, and regressive nuclear alterations. On the other hand, mice that had been concomitantly treated with BLF501 showed the maintenance of an almost physiological morphology of the lung parenchyma: only rare eosinophils are present in the alveolar septa, while the bronchial lumen is pervious. Immunohistochemical analysis, performed with anti-ICAM-1 and anti-caveolin antibodies, which represent markers of inflammation, showed that their expression was increased in mice treated with LPS alone, but comparable to controls in animals treated with BLF501 and LPS (Figure 3B,C).

Analysis of the bronchoalveolar lavage fluid (BALF) revealed that administration of LPS elicited a massive increase in total cell numbers, with neutrophils and macrophages representing the majority of cells, indicative of a significant inflammatory response. BLF501 treatment suppressed the accumulation of cells in the alveolar spaces (Table 1). The fluid phase of BALFs was analyzed for NO, a marker of cellular stress and damage [44]; high levels of NO were found in BALFs from LPS-treated mice (Supplementary Materials, Figure S4), while greatly reduced levels were present in animals that had been treated concomitantly with BLF501 (LPS 16.3 ± 2.0 µmol/mL; BLF501 5.3 ± 0.7 µmol/mL; LPS + BLF501 5.8 ± 1.1 µmol/mL; $p = 5.7 \times 10^{-8}$ vs. LPS). Altogether, these data suggest that BLF501 can lead to marked anti-inflammatory effects *in vivo*.

Table 1. Evaluation of neutrophil and macrophage infiltration in BALFs from LPS- and BLF501-treated mice (10 mice/group of treatment).

	Untr ¹	BLF501 ¹	LPS ¹	BLF501 + LPS ¹
Neutrophils	132/mL ± 13	122/mL ± 21	3500/mL ± 216	127/mL ± 28
Macrophages	36/mL ± 6	26/mL ± 7	350/mL ± 39	29/mL ± 11

¹ Data are reported as mean number of cells/mL BALF ± S.D.

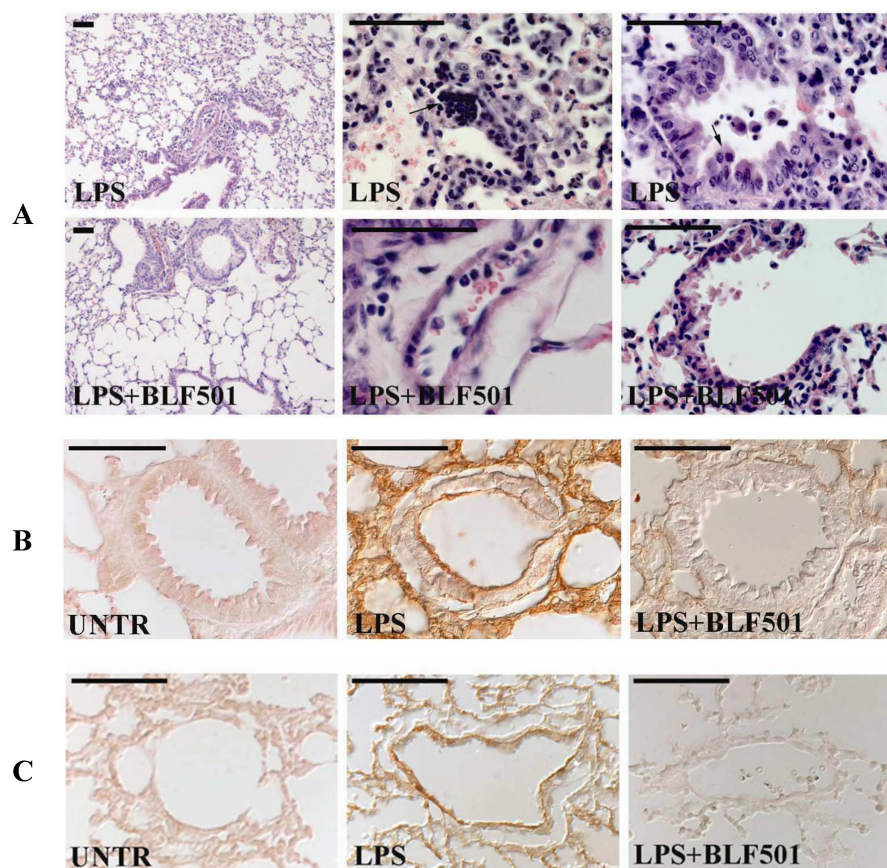


Figure 3. Aerosolized BLF501 protects the lungs from injury following aerosol administration of LPS. (A) Histological examination of the lung samples from mice exposed to LPS revealed significant inflammatory changes, including massive extravasation of leukocytes clustered in the alveolar spaces and proliferation areas in the bronchial epithelium (indicated by arrows). In contrast, the lung samples from mice treated with both BLF501 and LPS displayed normal lung parenchyma morphology. Scale bars: 50 μ m. (B,C) Immunohistochemical analysis using anti-ICAM-1 (B) and anti-caveolin (C) antibodies, both markers of inflammation, showed increased expression in mice treated with LPS alone. However, their expression levels were similar to the controls in mice treated with both BLF501 and LPS.

3.3. Anti-Inflammatory Effects of BLF501 in OVA-Induced Model of Allergic Asthma

The previous findings led us to investigate whether BLF501 could also inhibit other lung inflammatory conditions, such as allergic asthma. To explore this, we used a murine model of OVA-induced asthma, which results in pulmonary injury characterized by intense inflammation, marked eosinophilic cellular infiltration, and elevated levels of systemic TNF- α , IL-4, and IL-5 [45]. Asthma was induced by intraperitoneal (i.p.) immunization with 100 μ g OVA and 500 μ g aluminum hydroxide, followed by aerosol administration of 5% (wt/vol) OVA in two groups of mice (n = 10/group). One group also received concomitant aerosol administration of BLF501 (266 ng/mL, 3 mL).

Histological examination of the lungs showed the presence of marked cellular infiltration in tissues from OVA-treated animals, while mice concomitantly receiving BLF501 showed normal lung parenchyma (Figure 4). OVA-treated mice exhibited inflammatory cell aggregates surrounding the small blood arteries, with the infiltration closely adhering to the external vessel wall and no infiltration into the muscular tunica. Additionally, inflammatory infiltration composed of lymphocytes and eosinophils was observed along the external bronchial wall, while the lumen of mid-sized bronchi contained mucus with several erythrocytes. Significant inflammatory infiltration was also present in the alveolar septa, and the bronchial cylindrical epithelial cells showed notable hyperproliferation. In

contrast, mice treated with both BLF501 and OVA maintained a normal lung architecture, with no inflammatory infiltration in the vascular or bronchial regions, and the bronchial lumen was free of mucous secretory products (Figure 4). Analysis of the BALFs revealed a substantial increase in eosinophils in the lungs of OVA-treated mice (4103 ± 121 cells/mL), consistent with allergic asthma induction. However, mice treated with both BLF501 and OVA had eosinophil levels in their alveolar spaces (145 ± 24 cells/mL) comparable to those of untreated animals (157 ± 26 cells/mL).

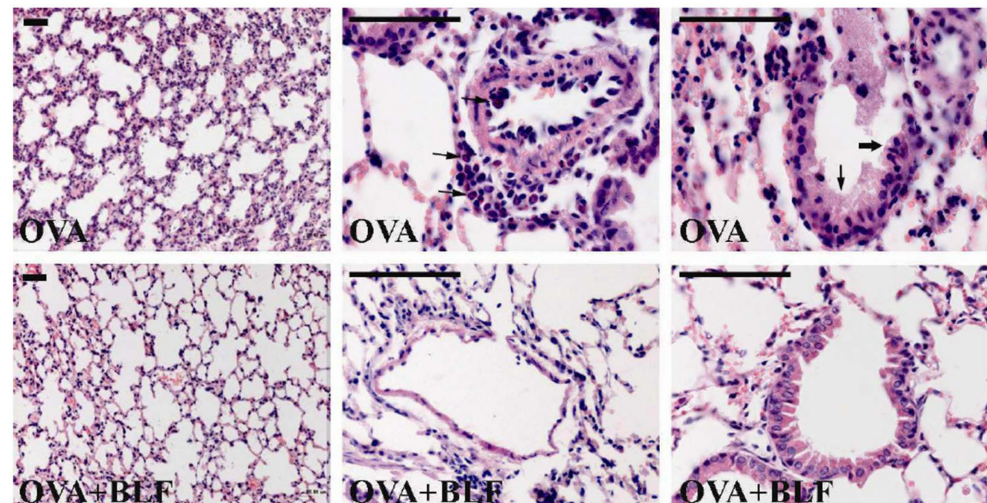


Figure 4. The effects of aerosolized BLF501 in the murine asthma model. Histological examination of the lungs of asthma model mice. The tissues of OVA-treated animals present cell aggregates grouped all around the small blood arteries, in strict contact with the wall of vessels (arrows); mid-dimensional bronchi are characterized by the presence of mucous (arrow) and epithelial hyperproliferation (full arrow). Mice concomitantly treated with BLF501 plus OVA showed normal lung parenchyma. Bars: 50 μ m.

A key indicator of inflammatory lung damage is the development of high-permeability edema, which is marked by a high protein content in the exudate. In fact, the protein concentration in the BALFs from the lungs of OVA-exposed mice was very high (0.729 ± 0.049 mg/mL). Conversely, the protein concentration in the BALFs from mice treated with both OVA and BLF501 was significantly lower (0.375 ± 0.038 mg/mL), similar to that of untreated animals (0.360 ± 0.054 mg/mL). Also, the NO levels in BALFs, which were 19.2 ± 1.9 μ mol/mL in OVA-treated mice, were reduced to 3.4 ± 0.5 μ mol/mL upon concomitant administration of BLF501, levels similar to those observed in untreated mice (2.9 ± 0.6 μ mol/mL). Eventually, we tested the serum and BALF content of different cytokines in control mice and mice at the end of the OVA or OVA plus BLF501 treatment. IL-5 and IL-4, key cytokines in allergic asthma, were elevated in both the sera (Figure 5A,B) and BALF of OVA-treated mice, but not in control mice or those treated with BLF501 plus OVA. Conversely, the anti-inflammatory cytokine IL-10 was significantly increased in the sera of mice treated with BLF501 plus OVA, while it remained similar to the control levels in mice treated with OVA alone (Figure 5D). Given that airway inflammation in asthma is associated with increased serum levels of IgE, we examined the levels of anti-OVA IgE in the sera of mice treated with aerosolized OVA, with or without BLF501. The levels of anti-OVA IgE were significantly higher in asthmatic mice compared to control mice. However, administration of BLF501 resulted in a significant reduction in these specific IgE levels (Figure 5C). Overall, these findings demonstrate that BLF501 has potent anti-inflammatory effects in an animal model of allergic asthma.

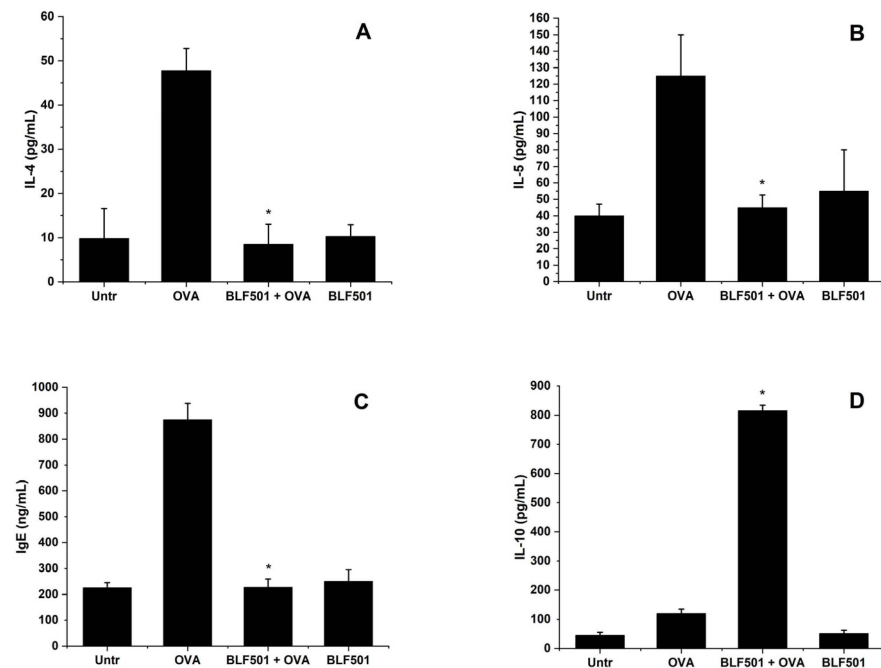


Figure 5. The anti-inflammatory effect of aerosolized BLF501 in an OVA-induced model of allergic asthma. (A,B) The ELISA results for IL-4 and IL-5, prototypical cytokines of allergic asthma: the levels of these cytokines were elevated in the sera of animals receiving OVA treatment, but not in untreated mice or mice treated with BLF501 plus OVA. The data are presented as mean values \pm S.D. ($n = 10/\text{group}$). * $p = 2.39 \times 10^{-7}$ vs. OVA (A) and $p = 1.01 \times 10^{-8}$ vs. OVA (B). (C) The ELISA results for anti-OVA IgE: the levels were significantly increased in OVA mice compared with those of untreated mice. Administration of BLF501 plus OVA maintained basal levels of these specific IgE sera. The data are presented as mean values \pm S.D. ($n = 10/\text{group}$). * $p = 7.65 \times 10^{-11}$ vs. OVA. (D) The ELISA results for IL-10: the levels of the anti-inflammatory cytokine IL-10 were greatly increased in the sera of mice treated with BLF501 plus OVA; in mice treated with OVA alone, the levels were similar to those in untreated animals. The data are presented as mean values \pm S.D. ($n = 10/\text{group}$). * $p = 1.59 \times 10^{-12}$ vs. OVA.

3.4. OVA-Induced Lung Inflammation Is Inhibited by Oral Administration of BLF501

SGLT1 is typically expressed by intestinal epithelial cells; in our previous work, we have shown that engagement of this transporter induces systemic production of protective anti-inflammatory cytokines [13]. Therefore, we investigated whether the anti-inflammatory effects of BLF501 might also be observed upon oral administration. Mice receiving OVA were orally treated or not with BLF501 (25 $\mu\text{g}/\text{kg}$). Serum, BALF, and lung samples were collected at the end of the treatments, and we performed the same determinations on these specimens as those for aerosolized BLF501. The results obtained were comparable to those obtained with aerosolized BLF501, as regards eosinophilic infiltration, serum and BALF protein content, cytokines, and anti-OVA IgE levels (Figure 6a,b), showing that BLF501 also protects against OVA-induced lung injury upon oral administration. It is noteworthy that p.o. administered BLF501 was as efficacious as aerosolized BLF501 in protecting against OVA-induced asthma, while intravenous BLF501 administration did not lead to any protective effect.

The literature indicates that the most important lung diseases, including chronic bronchitis, chronic obstructive pulmonary disease, acute lung injury, acute respiratory distress syndrome, and asthma, are all affected by TNF- α [46]. In fact, bacterial endotoxins are physiological stimuli for the synthesis of TNF- α , and in vivo administration of bacterial LPS induces high levels of TNF- α production in animal models; moreover, several pieces of evidence indicate that high levels of TNF- α are directly linked to asthmatic complications [46]. Therefore, we assessed the levels of this cytokine in our murine model of asthma following

BLF501 treatment. We performed a time-course experiment where we determined, over 1 month, the TNF- α levels in the sera of OVA-treated or OVA- and orally BLF501-treated mice. Mice treated with OVA alone exhibited two peaks of TNF- α on the 1st and 7th days of treatment, corresponding to the two sensitizations with OVA and aluminum hydroxide. The levels then remained steady at 100 pg/mL, before rising again from the 12th day during the 5 days of OVA aerosol administration, reaching approximately 230 pg/mL until day 22. Afterward, the TNF- α levels decreased but remained relatively high (80–200 pg/mL). In contrast, the OVA plus BLF501 group showed peak TNF- α levels at the same time points as the OVA-only group, but these levels were consistently much lower (Figure 6c).

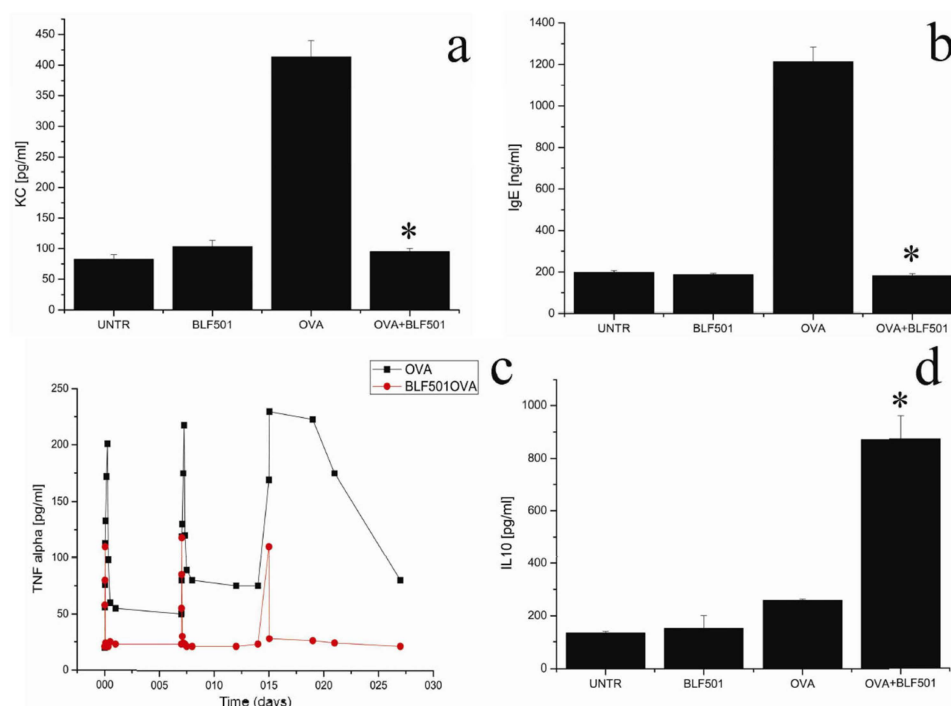


Figure 6. The effects of oral BLF501 in the murine asthma model and the involvement of dendritic cells. (a,b) The ELISA results for KC and anti-OVA IgE: BLF501 protects against OVA-induced lung injury upon oral administration. The levels of cytokines and IgE were elevated in the sera of animals receiving OVA treatment, but not in untreated mice or mice treated with BLF501 plus OVA. The data are presented as mean values \pm S.D. ($n = 10/\text{group}$). * $p = 7.25 \times 10^{-12}$ vs. OVA (a) and $p = 8.0 \times 10^{-13}$ vs. OVA. (c) The ELISA results for TNF- α in a time-course experiment: the OVA plus BLF501 (-●-) group presented peak levels of TNF- α at the same time points as the OVA-only group (-■-), but these were always much lower than in the OVA-only group. (d) The ELISA results for IL-10 levels in the supernatants of lung-derived CD11c+ cells. Cells were plated at the same cell density for all of the different treatment groups. The data are presented as mean values \pm S.D. * $p = 1.62 \times 10^{-9}$ vs. OVA.

We then went over to investigate the role of TNF- α in mice treated with OVA plus BLF501. For this purpose, we induced asthma in three groups of mice ($n = 10/\text{group}$): one group received only aerosolized OVA for 5 days; a second group received OVA plus BLF501; the third group received OVA, BLF501, and 5 μg of an anti-TNF- α neutralizing antibody, administered i.p. on the 4th and 5th day of OVA administration. Interestingly, the concomitant administration of the anti-TNF- α antibody blocked the protective effect of BLF501; the animals showed signs of inflammatory injury similar to those in OVA-treated mice, as revealed by morphological analysis and the evaluation of cytokine levels in BALFs and sera. In accordance with our previous work on liver inflammatory conditions [47], we observed that SGLT-1 activation was efficacious in triggering anti-inflammatory activity only in the presence of a danger signal; therefore, we focused our attention on discov-

ering which danger signal might be involved in the protection observed in the asthma model. These results point to a crucial role of circulating threshold levels of TNF- α as the second signal contributing to BLF501-effected protection in this OVA-induced model of allergic asthma.

3.5. Hsp27 Orchestrates the Anti-Inflammatory Effects of BLF501 Through the Induction of IL-10 Production by Dendritic Cells and Monocytes

We have reported above that the levels of the anti-inflammatory cytokine IL-10 were greatly increased in the sera of mice receiving BLF501 plus OVA, while they remained similar to the controls in mice treated with OVA alone. Therefore, the anti-inflammatory effects of BLF501 might be due to the production of an anti-inflammatory cytokine, such as IL-10, produced in response to the engagement of SGLT1, and a second signal, like TNF- α . Additionally, our previous works [47] demonstrated that the protective activity following SGLT-1 activation was abrogated in the presence of anti-IL-10 antibodies. For this reason, we set out to investigate in more detail the induction of systemic IL-10 production in response to BLF501. As reported above (Figure 6d), IL-10 showed only a slight increase in OVA-treated animals, while a marked increase was observed in mice treated with BLF501 and OVA. On the other hand, no IL-10 production was observed in untreated mice or mice treated only with BLF501. Monocytes and dendritic cells are known to be the main IL-10-producing cells [48]. This encouraged us to set up an experiment aimed at evaluating if dendritic cells and/or monocytes are involved in the increase in systemic IL-10 in response to OVA and BLF501. For this purpose, two groups of animals ($n = 10$ /group) were treated, as previously described, with OVA alone or with BLF501 plus OVA; untreated mice and mice treated only with BLF501 served as controls. At the end of treatment, lung samples were collected and pulmonary CD11c⁺ DCs were isolated by magnetic cell sorting. These cells were cultured at an equivalent cell density in vitro for 18 h; at the end of this period, supernatants were harvested for the determination of cytokines. These cells produced high levels of IL-10, greatly exceeding those from cells derived from the other groups (Figure 6d). Additionally, Table 2 shows that DCs obtained from mice treated with BLF501 plus OVA were significantly increased in number compared to the other groups, as revealed by cell count. This was confirmed by immunofluorescence experiments using an anti-CD11c antibody in lung samples.

Table 2. Evaluation of CD11c⁺ DCs isolated from lungs from OVA- and BLF501-treated mice (10 mice/group of treatment).

	Untr ¹	OVA ¹	BLF501 ¹	BLF501 + OVA ¹
CD11c + DCs	217 ± 35	360 ± 27	289 ± 52	4110 ± 328

¹ Data are reported as mean number of cells/lung ± S.D.

Since dendritic cells do not express SGLT1, they are unable to respond to BLF501 on their own. This suggests that DCs might receive a signal inducing IL-10 production, and this signal might be produced by epithelial cells, the only cells expressing SGLT1.

When asking which signal this might be, we considered data reporting that extracellular stress proteins, including hsp27, act as “danger signals” for the innate immune system [49] and induce anti-inflammatory mediators, such as IL-10 [50]. Therefore, we investigated whether hsp27 might represent the link between epithelial and DCs for the induction of IL-10 production. For this purpose, human colon carcinoma cells, HT-29, were stimulated with TNF- α in the absence or presence of BLF501, and supernatants were tested for the presence of hsp27. High levels of hsp27 were produced in response to TNF- α and BLF501 together, but not TNF- α or BLF501 alone (Figure 7a). To assess if BLF501-induced production of hsp27 was actually linked to the engagement of SGLT1, we repeated the experiments on HT-29 cells after treatment of the cells with anti-SGLT1 siRNA. Indeed, the silencing of the transporter completely blocked hsp27 production.

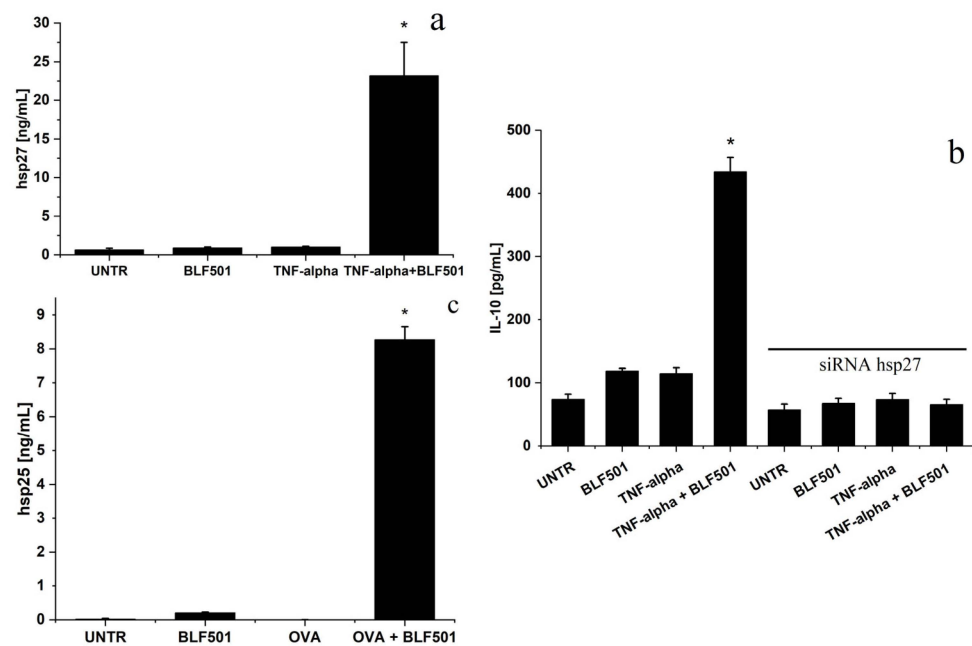


Figure 7. The role of hsp27/hsp25 in BLF501 activity. (a) The ELISA results for hsp27: high levels of hsp27 were produced by human colon carcinoma cells HT-29 in response to TNF- α plus BLF501, but not TNF- α or BLF501 alone. The data are presented as mean values \pm S.D. * $p = 3.90 \times 10^{-9}$ vs. TNF- α . (b) The ELISA results for IL-10 production by dendritic cells. In response to TNF- α and BLF501, enterocytes induced the production of high IL-10 levels by co-cultured DC cells. Pre-treatment with hsp27 siRNA blocked IL-10 production. The data are presented as mean values \pm S.D. * $p = 1.37 \times 10^{-11}$ vs. TNF- α . The knockdown efficiency of the hsp27 gene through silencing with siRNA was more than 75% (by qPCR analysis). (c) The ELISA results for hsp25: in accordance with the in vitro data, the sera from animals treated with OVA and BLF501 produced high amounts of hsp25 compared to untreated mice or mice treated with OVA alone. The data are presented as mean values \pm S.D. * $p = 2.45 \times 10^{-12}$ vs. OVA.

Together with dendritic cells, monocytes are also producers of IL-10 [48]. Therefore, a further experiment was performed in which HT-29 cells were co-cultured with human dendritic cells in order to assess whether hsp27 production by HT-29 cells in response to BLF501 plus TNF- α was able to induce IL-10 production by dendritic cells. Indeed, in response to TNF- α and BLF501, enterocytes induced the production of high IL-10 levels by co-cultured dendritic cells (Figure 7b); moreover, when HT-29 cells were silenced for hsp27 with siRNA, no IL-10 production was observed. In vivo, we assessed the production of hsp25, the murine analogue of human hsp27, in untreated mice or mice treated with OVA alone or OVA plus BLF501, as described in the Methods Section. In accordance with the in vitro data, the sera from animals treated with OVA and BLF501 produced high amounts of hsp25 compared to untreated mice or mice treated with OVA alone (Figure 7c).

4. Discussion

Multiple host factors are involved in regulating inflammation in the lungs, showing a protective role of the lung epithelium. Anti-inflammatory cytokines, such as IL-10, promote an effective immune response while also regulating inflammation to prevent excessive tissue damage [51]. Itaconate, a metabolite produced by macrophages, has significant anti-inflammatory and anti-oxidative stress properties in the lung epithelium [52,53]. Other well-known immune modulating factors that help maintain lung homeostasis include host antimicrobial peptides, which are secreted by epithelial cells; these peptides kill microorganisms directly while modulating immune responses and inflammation [54]. Surfactant proteins are produced by alveolar epithelial cells; these proteins enhance the phagocytosis

of pathogens by immune cells and modulate inflammatory responses, protecting lung tissue from excessive inflammation [55]. Toll-like receptors (TLRs) balance the immune response by promoting inflammation to fight infections while also activating anti-inflammatory pathways to prevent tissue damage [56].

In addition to the previously mentioned factors, the protective role of glucose in the lung epithelium under inflammatory and stress conditions is well documented. Glucose metabolism is essential for maintaining the alveolar epithelium, primarily through the expression of glucose transporter 1 (Glut-1), which is crucial for the proliferative capacity of airway progenitor cells [57]. Additionally, the activation of autophagy mechanisms supports the metabolism and regeneration of alveolar progenitor cells [58]. In this work, we highlight the significant protective role of SGLT1 in airway and alveolar inflammation and propose its involvement in protecting lung tissues under various pathological conditions. Our results show that in two experimental models, i.e., mice exposed to aerosolized LPS and OVA-induced asthma, the engagement of the glucose transporter SGLT1 induced potent anti-inflammatory effects in the lungs. As an SGLT1 ligand, the synthetic glucose analogue BLF501 was used, which emerged from *in vitro* screening aimed at identifying SGLT1 ligands which could lead to anti-inflammatory effects similar to those induced by glucose, but at much lower concentrations compatible with a possible therapeutic application.

In the first model analyzed in this paper, exposure to aerosolized LPS led to acute respiratory distress in mice, characterized by widespread destruction of the alveolar and endothelial epithelia and flooding of the alveolar spaces with protein-rich exudates containing large numbers of neutrophils [59–61]. This occurs due to LPS binding to pattern recognition receptors, which triggers the expression of pro-inflammatory cytokines (TNF- α and IL-1 β), chemokines (KC or IL-8), and adhesion molecules (ICAM-1 and VCAM-1). These molecules facilitate the extravasation of neutrophils across the endothelial and epithelial barriers that separate the bloodstream from the pulmonary air spaces [62–64]. In contrast, mice treated with both LPS and aerosolized BLF501 exhibited normal lung parenchyma, with no cellular deposits within the alveoli, and their serum levels of KC, IL-12, and IFN- γ were similar to those of untreated mice. Immunohistochemical analysis of lung sections showed a significant increase in ICAM-1 and caveolin expression in mice treated with LPS alone, but not in those treated with both LPS and BLF501. Additionally, analysis of the BALFs revealed high levels of NO in LPS-treated animals, but not in those also treated with BLF501. Notably, the engagement of SGLT1 by BLF501 alone did not affect inflammatory parameters, as mice receiving only BLF501 were comparable to untreated control mice.

BLF501 demonstrated similar protective effects in OVA-induced allergic asthma. Although the pathogenesis of this model differs significantly from LPS-induced lung injury, both share similar inflammatory outcomes, such as abundant cellular infiltration in the lung parenchyma and elevated serum levels of pro-inflammatory chemokines and cytokines. Lung tissue from BLF501-treated mice showed no alveolar lymphocyte or blood infiltration and no accumulation of neutrophils or eosinophils in the BALFs. The reduction in leukocyte infiltration observed in mice treated with both OVA and BLF501 likely plays a crucial role in the anti-inflammatory effects seen in this context, as neutrophils are primary effector cells in the alveolo-capillary damage associated with lung inflammation [65]. Regarding cytokines, mice treated with OVA alone had high levels of IL-4 and IL-5, which are key cytokines in asthma pathogenesis. In contrast, mice treated with both BLF501 and OVA had normal levels of IL-4 and IL-5, while the anti-inflammatory cytokine IL-10 was significantly increased. Additionally, IgE serum levels, which were elevated in OVA-treated mice, returned to baseline levels in mice co-administered with BLF501.

The BALFs from mice treated with OVA alone showed a high protein content, indicating high-permeability pulmonary edema. In contrast, the protein concentration in the BALFs from BLF501-treated mice was similar to that of untreated mice or those treated with BLF501 alone. This indicates that BLF501 effectively reduced abnormal lung vascular permeability and promoted the resolution of lung edema, suggesting that BLF501 helps maintain the integrity of the alveolo-capillary membrane.

We observed that orally administered BLF501 and aerosolized BLF501 have a protective activity in OVA-induced asthma, while intravenous BLF501 administration did not lead to any protective effect. These findings suggest that oral administration of BLF501 engages SGLT-1 expressed in intestinal epithelial cells, leading to the direct or indirect release of an anti-inflammatory molecule.

Mice treated with BLF501 and OVA exhibited very high systemic levels of the anti-inflammatory cytokine IL-10. This cytokine, primarily produced by dendritic cells (DCs) and monocytes, is a typical anti-inflammatory mediator [48]. Administration of recombinant IL-10 has been shown to improve survival in mice with sepsis, and IL-10 gene therapy significantly reduces sepsis-induced multi-organ failure [66]. Therefore, IL-10 produced by DCs and monocytes likely serves as the final mediator of the systemic anti-inflammatory effects induced by BLF501. Although DCs do not express SGLT1, they produce IL-10 when activated by hsp27 [50,67], and our *in vitro* data showed that hsp27, or its murine homologous hps25, is strongly secreted by SGLT1-positive epithelial cells upon stimulation with BLF501 in the presence of an inflammatory stimulus. Moreover, co-culture of A549 pneumocytes and DCs led to the production of high levels of IL-10 by DCs. In A549 cells, stimulated with BLF501 plus an inflammatory agent, SGLT1 was activated and a large amount of hsp27 was secreted and released in a basolateral culture medium. DCs co-cultured and stimulated by hsp27 produced IL-10. This production was eliminated upon the silencing of SGLT-1 expression in pneumocytes. *In vivo*, a strong increase in hsp25 serum levels was observed when mice were treated with OVA and BLF501. Altogether, these findings strongly suggest hsp25/hsp27 as a mediator of the activation of SGLT1 and the production of IL-10 by dendritic cells.

Several studies confirm that hsp27 acts as an extracellular anti-inflammatory signal protein, often referred to as an “anti-danger signal”. These studies report that hsp27 is responsible for inducing IL-10, which in turn triggers significant immunoregulatory activity. Hsp27 has been shown to induce an anti-inflammatory response through IL-10 production in human monocytes [68,69]. According to De et al., the induction of IL-10 production by human monocytes involves the activation of the MAPK-p38 pathway [69]. Similarly, Salari et al. observed that hsp27 triggers IL-10 expression in macrophages, mediated by the activation of the transcription factor NF- κ B [70]. In macrophages, NF- κ B signaling activation by hsp27 is associated with a balance in the expression and secretion of key pro- and anti-inflammatory cytokines, which are fundamental to the inflammation processes in atherosclerosis [71]. Various cell membrane receptors, such as CD or Toll-like receptors (TLRs), could be targets for exogenous HSPs [71]. Rayner et al. reported that exogenous hsp27 binds to TLR4, leading to the activation of the NF- κ B pathway, which controls the production of pro- and anti-inflammatory cytokines, including IL-10 [72]. More recently, the same group highlighted the role of the hsp27 immune complex (IC), a complex between hsp27 and its IgG auto-antibodies, in attenuating inflammation signaling in macrophages that regulate atherosclerosis [73]. In this case, the interaction between hsp27 IC and TLR4 leads to the activation of the NF- κ B signaling pathway. Therefore, according to our findings, the most plausible hypothesis is that hsp27, exhibiting a similar behavior in our models of lung inflammation, interacts with TLR4 expressed on dendritic cells (DCs), inducing IL-10 production.

The evidence of the great production of hsp27 and its extracellular secretion led us to detect a transcription factor probably involved in hsp27 expression in an attempt to connect SGLT1 activation with hsp production. Asthma is described as an NF- κ B-dependent pathology [74]. Several lines of evidence indicate enhanced NF- κ B pathway activation in various asthmatic tissues; bronchial epithelial cells and alveolar macrophages for example have greater levels of NF- κ B p65 and p50 activation [75,76].

Current asthma therapies act against both epithelial and immune cells blocking NF- κ B pathway activation, including a reduction in pro-inflammatory cytokine production and a decrease in IL-10. This complex of events describes an immunosuppressive status that could promote side effects like bacterial infections (typical side effects of asthma therapy).

In our work, we noticed the strong inhibition of the NF- κ B pathway in epithelial cells via SGLT1 activation. On the contrary, we also noticed the concomitant activation of immune cells via hsp27 with IL-10 production. In fact, in immune cells that do not express SGLT1, BLF501 could not inhibit the NF- κ B pathway.

5. Conclusions

In conclusion, the findings of this work suggest the engagement of SGLT1 in lung inflammation processes; both in vitro and in vivo experiments clearly indicated a protective anti-inflammatory effect upon engagement of this glucose co-transporter. The presented results, showing that BLF501 exerts potent anti-inflammatory effects in two different experimental models of inflammatory lung diseases, provide direction on a new pharmacological approach for the treatment of inflammatory lung diseases. Thus, the synthetic SGLT1 ligand, a glucose derivative BLF501, might represent a drug candidate for therapeutic intervention against lung inflammation and in particular allergic asthma, a disease of increasing worldwide prevalence and representing a still unmet clinical need.

Supplementary Materials: The following supporting information can be downloaded at: <https://www.mdpi.com/article/10.3390/immuno4040031/s1>, Figure S1: Dose–response experiment of aerosol LPS- and BLF501-exposed mice; Figure S2: D-glucose and BLF501 inhibition of Nitric Oxide (NO) production (an LPS-induced response) in A549 cells; Figure S3. Immunofluorescence analysis of SGLT1 expression in normal murine lungs; Figure S4: NO levels in BALFs.

Author Contributions: Conceptualization, C.R., G.D. (Giuseppina Dusio), B.L.F.; methodology, G.D. (Giuseppina Dusio), D.C.; validation, G.D. (Giuseppina Dusio); investigation, C.R., D.C., G.D. (Giuseppina Dusio), G.D. (Giuseppe D’Orazio); writing—original draft preparation, G.D. (Giuseppina Dusio), C.R., G.D. (Giuseppe D’Orazio); writing—review and editing, G.D. (Giuseppina Dusio), C.R., B.L.F., G.D. (Giuseppe D’Orazio); supervision, C.R. All authors have read and agreed to the published version of the manuscript.

Funding: This research received no external funding.

Institutional Review Board Statement: All experiments on animals were conducted following the Italian and European Community Council for Animal Care (2010/63/EU) guidelines and regulations; the experimental protocols were approved by the Ethics Committee for Animal Experimentation of the Istituto Nazionale dei Tumori (INT) (Milan, Italy) according to UKCCCR guidelines.

Informed Consent Statement: Not applicable.

Data Availability Statement: The data are contained within this article or the Supplementary Materials.

Conflicts of Interest: The authors declare no conflicts of interest.

Abbreviations

SGLT1: sodium–glucose co-transporter 1; TLRs: Toll-like receptors; BALFs: broncho-alveolar lavage fluids; LPS: Lipopolysaccharide; siRNA: small interfering RNA; NO: Nitric Oxide; OVA: ovalbumin; TNF α : Tumor necrosis factor α ; IL: Interleukin; Hsp27: Heat shock protein 27; ICAM-1: Intercellular Adhesion Molecule 1; VCAM-1: Vascular Cell Adhesion Molecule 1; KC: Keratinocyte chemoattractant; IFN γ : Interferon γ ; DC: dendritic cell.

References

1. Horby, P.; Lim, W.S.; Emberson, J.R.; Mafham, M.; Bell, J.L.; Linsell, L.; Staplin, N.; Brightling, C.; Ustianowski, A.; Elmahi, E.; et al. Dexamethasone in Hospitalized Patients with COVID-19. *N. Engl. J. Med.* **2021**, *384*, 693–704. [[CrossRef](#)] [[PubMed](#)]
2. Pasrija, R.; Naime, M. The deregulated immune reaction and cytokines release storm (CRS) in COVID-19 disease. *Int. Immunopharmacol.* **2021**, *90*, 107225. [[CrossRef](#)] [[PubMed](#)]
3. Coperchini, F.; Chiovato, L.; Croce, L.; Magri, F.; Rotondi, M. The cytokine storm in COVID-19: An overview of the involvement of the chemokine/chemokine-receptor system. *Cytokine Growth Factor Rev.* **2020**, *53*, 25–32. [[CrossRef](#)] [[PubMed](#)]
4. Tay, M.Z.; Poh, C.M.; Renia, L.; MacAry, P.A.; Ng, L.F.P. The trinity of COVID-19: Immunity, inflammation and intervention. *Nat. Rev. Immunol.* **2020**, *20*, 363–374. [[CrossRef](#)]

5. Chignard, M.; Balloy, V. Neutrophil recruitment and increased permeability during acute lung injury induced by lipopolysaccharide. *Am. J. Physiol. Lung Cell. Mol. Physiol.* **2000**, *279*, L1083–L1090. [[CrossRef](#)]
6. Shinbori, T.; Walczak, H.; Krammer, P.H. Activated T killer cells induce apoptosis in lung epithelial cells and the release of pro-inflammatory cytokine TNF-alpha. *Eur. J. Immunol.* **2004**, *34*, 1762–1770. [[CrossRef](#)]
7. Wright, M.M.; Powell, C.S.; Jackson, R.M. Effects of intratracheal tumor necrosis factor-alpha plasmid vector on lipopolysaccharide lethality and lung injury in mice. *Exp. Lung Res.* **2004**, *30*, 653–671. [[CrossRef](#)]
8. Haddad, I.Y.; Pataki, G.; Hu, P.; Galliani, C.; Beckman, J.S.; Matalon, S. Quantitation of Nitrotyrosine Levels in Lung Sections of Patients and Animals with Acute Lung Injury. *J. Clin. Investig.* **1994**, *94*, 2407–2413. [[CrossRef](#)]
9. Matthay, M.A.; Geiser, T.; Matalon, S.; Ischiropoulos, H. Oxidant-mediated lung injury in the acute respiratory distress syndrome. *Crit. Care Med.* **1999**, *27*, 2028–2030. [[CrossRef](#)]
10. Dorger, M.; Allmeling, A.M.; Kieffmann, R.; Munzing, S.; Messmer, K.; Krombach, F. Early inflammatory response to asbestos exposure in rat and hamster lungs: Role of inducible nitric oxide synthase. *Toxicol. Appl. Pharmacol.* **2002**, *181*, 93–105. [[CrossRef](#)]
11. Greene, C.M.; McElvaney, N.G. Toll-like receptor expression and function in airway epithelial cells. *Arch. Immunol. Ther. Exp.* **2005**, *53*, 418–427.
12. Koff, J.L.; Shao, M.X.G.; Ueki, I.F.; Nadel, J.A. Multiple TLRs activate EGFR via a signaling cascade to produce innate immune responses in airway epithelium. *Am. J. Physiol.-Lung Cell. Mol. Physiol.* **2008**, *294*, L1068–L1075. [[CrossRef](#)] [[PubMed](#)]
13. Palazzo, M.; Gariboldi, S.; Zanoibio, L.; Selli, S.; Dusio, G.F.; Mauro, V.; Rossini, A.; Balsari, A.; Rumio, C. Sodium-dependent glucose transporter-1 as a novel immunological player in the intestinal mucosa. *J. Immunol.* **2008**, *181*, 3126–3136. [[CrossRef](#)] [[PubMed](#)]
14. Koepsell, H. Glucose transporters in the small intestine in health and disease. *Pflug. Arch. Eur. J. Physiol.* **2020**, *472*, 1207–1248. [[CrossRef](#)]
15. Mamchaoui, K.; Makhoulfi, Y.; Saumon, G. Glucose transporter gene expression in freshly isolated and cultured rat pneumocytes. *Acta Physiol. Scand.* **2002**, *175*, 19–24. [[CrossRef](#)]
16. Bodega, F.; Sironi, C.; Armilli, M.; Porta, C.; Agostoni, E. Evidence for Na⁺-glucose cotransporter in type I alveolar epithelium. *Histochem. Cell Biol.* **2010**, *134*, 129–136. [[CrossRef](#)]
17. Vrhovac, I.; Erer, D.B.; Klessen, D.; Burger, C.; Breljak, D.; Kraus, O.; Radovic, N.; Jadrijevic, S.; Aleksic, I.; Walles, T.; et al. Localizations of Na⁺-D-glucose cotransporters SGLT1 and SGLT2 in human kidney and of SGLT1 in human small intestine, liver, lung, and heart. *Pflug. Arch. Eur. J. Physiol.* **2015**, *467*, 1881–1898. [[CrossRef](#)]
18. Cardoso-Sousa, L.; Aguiar, E.M.G.; Caixeta, D.C.; Vilela, D.D.; da Costa, D.P.; Silva, T.L.; Cunha, T.M.; Faria, P.R.; Espindola, F.S.; Jardim, A.C.; et al. Effects of salbutamol and phlorizin on acute pulmonary inflammation and disease severity in experimental sepsis. *PLoS ONE* **2019**, *14*, e0222575. [[CrossRef](#)]
19. Oliveira, T.L.; Candeia-Medeiros, N.; Cavalcante-Araujo, P.M.; Melo, I.S.; Favaro-Pipi, E.; Fatima, L.A.; Rocha, A.A.; Goulart, L.R.; Machado, U.F.; Campos, R.R.; et al. SGLT1 activity in lung alveolar cells of diabetic rats modulates airway surface liquid glucose concentration and bacterial proliferation. *Sci. Rep.* **2016**, *6*, 21752. [[CrossRef](#)]
20. Sharma, P.; Khairnar, V.; Madunic, I.V.; Singh, Y.; Pandya, A.; Salker, M.S.; Koepsell, H.; Sabolic, I.; Lang, F.; Lang, P.A.; et al. SGLT1 Deficiency Turns Listeria Infection into a Lethal Disease in Mice. *Cell. Physiol. Biochem.* **2017**, *42*, 1358–1365. [[CrossRef](#)]
21. La Ferla, B.; Spinosa, V.; D’Orazio, G.; Palazzo, M.; Balsari, A.; Foppoli, A.A.; Rumio, C.; Nicotra, F. Dansyl C-glucoside as a novel agent against endotoxic shock. *ChemMedChem* **2010**, *5*, 1677–1680. [[CrossRef](#)] [[PubMed](#)]
22. Nicotra, F.; Airoidi, C.; Cardona, F.; Johannis, P.K. Synthesis of C- and S-Glycosides. In *Comprehensive Glycoscience*; Elsevier: Oxford, UK, 2007; pp. 647–683.
23. Paiotta, A.; D’Orazio, G.; Palorini, R.; Ricciardiello, F.; Zoia, L.; Votta, G.; De Gioia, L.; Chiaradonna, F.; La Ferla, B. Design, Synthesis, and Preliminary Biological Evaluation of GlcNAc-6P Analogues for the Modulation of Phosphoacetylglucosamine Mutase 1 (AGM1/PGM3). *Eur. J. Org. Chem.* **2018**, *2018*, 1946–1952. [[CrossRef](#)]
24. Ernst, B.; Magnani, J.L. From carbohydrate leads to glycomimetic drugs. *Nat. Rev. Drug Discov.* **2009**, *8*, 661–677. [[CrossRef](#)] [[PubMed](#)]
25. Ricciardiello, F.; Votta, G.; Palorini, R.; Raccagni, I.; Brunelli, L.; Paiotta, A.; Tinelli, F.; D’Orazio, G.; Valtorta, S.; De Gioia, L.; et al. Inhibition of the Hexosamine Biosynthetic Pathway by targeting PGM3 causes breast cancer growth arrest and apoptosis. *Cell Death Dis.* **2018**, *9*, 377. [[CrossRef](#)]
26. D’Orazio, G.; Parisi, G.; Policano, C.; Mechelli, R.; Pisanelli, G.C.; Pitaro, M.; Ristori, G.; Salvetti, M.; Nicotra, F.; La Ferla, B. Arsenical C-Glucoside Derivatives with Promising Antitumor Activity. *Eur. J. Org. Chem.* **2015**, *2015*, 4620–4623. [[CrossRef](#)]
27. Nicotra, F.; Cipolla, L.; La Ferla, B.; Airoidi, C.; Zona, C.; Orsato, A.; Shaikh, N.; Russo, L. Carbohydrate scaffolds in chemical genetic studies. *J. Biotechnol.* **2009**, *144*, 234–241. [[CrossRef](#)]
28. Tamburrini, A.; Colombo, C.; Bernardi, A. Design and synthesis of glycomimetics: Recent advances. *Med. Res. Rev.* **2020**, *40*, 495–531. [[CrossRef](#)]
29. Hevey, R. Strategies for the Development of Glycomimetic Drug Candidates. *Pharmaceuticals* **2019**, *12*, 55. [[CrossRef](#)]
30. Fernández-Tejada, A.; Cañada, F.J.; Jiménez-Barbero, J. Recent Developments in Synthetic Carbohydrate-Based Diagnostics, Vaccines, and Therapeutics. *Chem. Eur. J.* **2015**, *21*, 10616–10628. [[CrossRef](#)]
31. Compain, P.; Martin, O.R. Carbohydrate mimetics-based glycosyltransferase inhibitors. *Bioorg. Med. Chem.* **2001**, *9*, 3077–3092. [[CrossRef](#)]

32. Barchi, J.J. Emerging roles of carbohydrates and glycomimetics in anticancer drug design. *Curr. Pharm. Des.* **2000**, *6*, 485–501. [[CrossRef](#)] [[PubMed](#)]
33. Filice, M.; Palomo, J.M. Monosaccharide derivatives as central scaffolds in the synthesis of glycosylated drugs. *RSC Adv.* **2012**, *2*, 1729–1742. [[CrossRef](#)]
34. D’Orazio, G.; Martorana, A.M.; Filippi, G.; Polissi, A.; Gioia, L.D.; Ferla, B.L. N-Spiro-fused Bicyclic Derivatives of 1-Deoxynojirimycin: Synthesis and Preliminary Biological Evaluation. *ChemistrySelect* **2016**, *1*, 2444–2447. [[CrossRef](#)]
35. Cardani, D.; Sardi, C.; La Ferla, B.; D’Orazio, G.; Sommariva, M.; Marcucci, F.; Olivero, D.; Tagliabue, E.; Koepsell, H.; Nicotra, F.; et al. Sodium glucose cotransporter 1 ligand BLF501 as a novel tool for management of gastrointestinal mucositis. *Mol. Cancer* **2014**, *13*, 23. [[CrossRef](#)]
36. D’Orazio, G.; Marradi, M.; La Ferla, B. Dual-Targeting Gold Nanoparticles: Simultaneous Decoration with Ligands for Co-Transporters SGLT-1 and B0AT1. *Appl. Sci.* **2024**, *14*, 2248. [[CrossRef](#)]
37. Giudicelli, J.; Bertrand, M.F.; Bilski, S.; Tran, T.T.; Poiree, J.C. Effect of cross-linkers on the structure and function of pig-renal sodium-glucose cotransporters after papain treatment. *Biochem. J.* **1998**, *330*, 733–736. [[CrossRef](#)]
38. Stevens, B.R.; Fernandez, A.; Hirayama, B.; Wright, E.M.; Kempner, E.S. Intestinal Brush-Border Membrane Na⁺/Glucose Cotransporter Functions In situ as a Homotetramer. *Proc. Natl. Acad. Sci. USA* **1990**, *87*, 1456–1460. [[CrossRef](#)]
39. Takahashi, M.; Malathi, P.; Preiser, H.; Jung, C.Y. Radiation Inactivation Studies on the Rabbit Kidney Sodium-Dependent Glucose Transporter. *J. Biol. Chem.* **1985**, *260*, 551–556. [[CrossRef](#)]
40. Turner, R.J.; Kempner, E.S. Radiation Inactivation Studies of the Renal Brush-Border Membrane Phlorizin-Binding Protein. *J. Biol. Chem.* **1982**, *257*, 794–797. [[CrossRef](#)]
41. Dusio, G. Immunomodulation and Intestinal Barrier Protection Activities of a Novel Synthetic Glucose Analogue in Inflammatory Animal Model of Colitis and Asthma. Ph.D. Thesis, University of Milan, Milan, Italy, 2010.
42. Tiruppathi, C.; Shimizu, J.; Miyawaki-Shimizu, K.; Vogel, S.M.; Bair, A.M.; Minshall, R.D.; Predescu, D.; Malik, A.B. Role of NF- κ B-dependent caveolin-1 expression in the mechanism of increased endothelial permeability induced by lipopolysaccharide. *J. Biol. Chem.* **2008**, *283*, 4210–4218. [[CrossRef](#)]
43. Wang, H.; Cheng, C.; Qin, Y.; Niu, S.; Gao, S.; Li, X.; Tao, T.; Shen, A. Role of Mitogen-Activated Protein Kinase Cascades in Inducible Nitric Oxide Synthase Expression by Lipopolysaccharide in a Rat Schwann Cell Line. *Neurochem. Res.* **2009**, *34*, 430–437. [[CrossRef](#)] [[PubMed](#)]
44. Wu, T.-L.; Chang, P.-Y.; Tsao, K.-C.; Sun, C.-F.; Wu, L.L.; Wu, J.T. A panel of multiple markers associated with chronic systemic inflammation and the risk of atherogenesis is detectable in asthma and chronic obstructive pulmonary disease. *J. Clin. Lab. Anal.* **2007**, *21*, 367–371. [[CrossRef](#)] [[PubMed](#)]
45. Hessel, E.M.; VanOosterhout, A.J.M.; VanArk, I.; VanEsch, B.; Hofman, G.; VanLoveren, H.; Savelkoul, H.F.J.; Nijkamp, F.P. Development of airway hyperresponsiveness is dependent on interferon-gamma and independent of eosinophil infiltration. *Am. J. Respir. Cell Mol. Biol.* **1997**, *16*, 325–334. [[CrossRef](#)] [[PubMed](#)]
46. Mukhopadhyay, S.; Hoidal, J.R.; Mukherjee, T.K. Role of TNF alpha in pulmonary pathophysiology. *Respir. Res.* **2006**, *7*, 125. [[CrossRef](#)]
47. Zanolibio, L.; Palazzo, M.; Gariboldi, S.; Dusio, G.F.; Cardani, D.; Mauro, V.; Marcucci, F.; Balsari, A.; Rumio, C. Intestinal Glucose Uptake Protects Liver from Lipopolysaccharide and D-Galactosamine, Acetaminophen, and Alpha-Amanitin in Mice. *Am. J. Pathol.* **2009**, *175*, 1066–1076. [[CrossRef](#)]
48. Ogawa, Y.; Duru, E.A.; Ameredes, B.T. Role of IL-10 in the resolution of airway inflammation. *Curr. Mol. Med.* **2008**, *8*, 437–445. [[CrossRef](#)]
49. Wheeler, D.S.; Wong, H.R. Heat shock response and acute lung injury. *Free Radic. Biol. Med.* **2007**, *42*, 1–14. [[CrossRef](#)]
50. Laudanski, K.; De, A.; Miller-Graziano, C. Exogenous heat shock protein 27 uniquely blocks differentiation of monocytes to dendritic cells. *Eur. J. Immunol.* **2007**, *37*, 2812–2824. [[CrossRef](#)]
51. Gopallawa, I.; Dehinwal, R.; Bhatia, V.; Gujar, V.; Chirmule, N. A four-part guide to lung immunology: Invasion, inflammation, immunity, and intervention. *Front. Immunol.* **2023**, *14*, 1119564. [[CrossRef](#)]
52. He, R.; Zuo, Y.; Yi, K.; Liu, B.; Song, C.; Li, N.; Geng, Q. The role and therapeutic potential of itaconate in lung disease. *Cell. Mol. Biol. Lett.* **2024**, *29*, 129. [[CrossRef](#)]
53. Michalaki, C.; Albers, G.J.; Byrne, A.J. Itaconate as a key regulator of respiratory disease. *Clin. Exp. Immunol.* **2024**, *215*, 120–125. [[CrossRef](#)] [[PubMed](#)]
54. Lafferty, E.L.; Qureshi, S.T.; Schnare, M. The role of toll-like receptors in acute and chronic lung inflammation. *J. Inflamm.* **2010**, *7*, 57. [[CrossRef](#)] [[PubMed](#)]
55. Borchers, M.T.; Lau, G.W.; Dela Cruz, C.S. Editorial: Outsmarting the Host: How Bacterial Pathogens Modulate Immune Responses in the Lung. *Front. Immunol.* **2020**, *11*, 629491. [[CrossRef](#)]
56. Marrella, V.; Nicchiotti, F.; Cassani, B. Microbiota and Immunity during Respiratory Infections: Lung and Gut Affair. *Int. J. Mol. Sci.* **2024**, *25*, 4051. [[CrossRef](#)]
57. Li, K.; Li, M.; Li, W.; Yu, H.; Sun, X.; Zhang, Q.; Li, Y.; Li, X.; Abel, E.D.; Wu, Q.; et al. Airway epithelial regeneration requires autophagy and glucose metabolism. *Cell Death Dis.* **2019**, *10*, 875. [[CrossRef](#)]
58. Li, X.; Wu, J.; Sun, X.; Wu, Q.; Li, Y.; Li, K.; Zhang, Q.; Abel, E.D.; Chen, H. Autophagy Reprograms Alveolar Progenitor Cell Metabolism in Response to Lung Injury. *Stem Cell Rep.* **2020**, *14*, 420–432. [[CrossRef](#)]

59. Bachofen, M.; Weibel, E.R. Structural alterations of lung parenchyma in the adult respiratory distress syndrome. *Clin. Chest Med.* **1982**, *3*, 35–56. [[CrossRef](#)]
60. Kline, J.N.; Cowden, J.D.; Hunninghake, G.W.; Schutte, B.C.; Watt, J.L.; Wohlford-Lenane, C.L.; Powers, L.S.; Jones, M.P.; Schwartz, D.A. Variable airway responsiveness to inhaled lipopolysaccharide. *Am. J. Respir. Crit. Care Med.* **1999**, *160*, 297–303. [[CrossRef](#)]
61. Arbour, N.C.; Lorenz, E.; Schutte, B.C.; Zabner, J.; Kline, J.N.; Jones, M.; Frees, K.; Watt, J.L.; Schwartz, D.A. TLR4 mutations are associated with endotoxin hyporesponsiveness in humans. *Nat. Genet.* **2000**, *25*, 187–191. [[CrossRef](#)]
62. Chollet-Martin, S. Polymorphonuclear neutrophil activation during the acute respiratory distress syndrome. *Intensive Care Med.* **2000**, *26*, 1575–1577. [[CrossRef](#)]
63. Martin, M.A.; Silverman, H.J. Gram-Negative Sepsis and the Adult Respiratory-Distress Syndrome. *Clin. Infect. Dis.* **1992**, *14*, 1213–1228. [[CrossRef](#)] [[PubMed](#)]
64. Puneet, P.; Moochhala, S.; Bhatia, M. Chemokines in acute respiratory distress syndrome. *Am. J. Physiol. Lung Cell. Mol. Physiol.* **2005**, *288*, L3–L15. [[CrossRef](#)] [[PubMed](#)]
65. Davidson, K.G.; Bersten, A.D.; Barr, H.A.; Dowling, K.D.; Nicholas, T.E.; Doyle, I.R. Lung function, permeability, and surfactant composition in oleic acid-induced acute lung injury in rats. *Am. J. Physiol. Lung Cell. Mol. Physiol.* **2000**, *279*, L1091–L1102. [[CrossRef](#)]
66. Howard, M.; Muchamuel, T.; Andrade, S.; Menon, S. Interleukin-10 Protects Mice from Lethal Endotoxemia. *J. Exp. Med.* **1993**, *177*, 1205–1208. [[CrossRef](#)]
67. Xu, W.; Schlagwein, N.; Roos, A.; van den Berg, T.K.; Daha, M.R.; van Kooten, C. Human peritoneal macrophage show functional characteristics of M-CSF-driven anti-inflammatory type 2 macrophages. *Eur. J. Immunol.* **2007**, *37*, 1594–1599. [[CrossRef](#)]
68. Miller-Graziano, C.L.; De, A.; Laudanski, K.; Herrmann, T.; Bandyopadhyay, S. HSP27: An anti-inflammatory and immunomodulatory stress protein acting to dampen immune function. In *The Biology of Extracellular Molecular Chaperones: Novartis Foundation Symposium 291*; Wiley: Hoboken, NJ, USA, 2008; pp. 196–294. [[CrossRef](#)]
69. De, A.K.; Kodys, K.M.; Yeh, B.S.; Miller-Graziano, C. Exaggerated human monocyte IL-10 concomitant to minimal TNF-alpha induction by heat-shock protein 27 (Hsp27) suggests Hsp27 is primarily an antiinflammatory stimulus. *J. Immunol.* **2000**, *165*, 3951–3958. [[CrossRef](#)]
70. Salari, S.; Seibert, T.; Chen, Y.X.; Hu, T.; Shi, C.; Zhao, X.; Cuerrier, C.M.; Raizman, J.E.; O'Brien, E.R. Extracellular HSP27 acts as a signaling molecule to activate NF- κ B in macrophages. *Cell Stress Chaperones* **2013**, *18*, 53–63. [[CrossRef](#)]
71. Batulan, Z.; Pulakazhi Venu, V.K.; Li, Y.; Koumbadinga, G.; Alvarez-Olmedo, D.G.; Shi, C.; O'Brien, E.R. Extracellular Release and Signaling by Heat Shock Protein 27: Role in Modifying Vascular Inflammation. *Front. Immunol.* **2016**, *7*, 285. [[CrossRef](#)]
72. Rayner, K.; Sun, J.; Chen, Y.X.; McNulty, M.; Simard, T.; Zhao, X.; Wells, D.J.; de Belleruche, J.; O'Brien, E.R. Heat shock protein 27 protects against atherogenesis via an estrogen-dependent mechanism: Role of selective estrogen receptor beta modulation. *Arterioscler. Thromb. Vasc. Biol.* **2009**, *29*, 1751–1756. [[CrossRef](#)]
73. Shi, C.; Deng, J.; Chiu, M.; Chen, Y.X.; O'Brien, E.R. Heat shock protein 27 immune complex altered signaling and transport (ICAST): Novel mechanisms of attenuating inflammation. *FASEB J.* **2020**, *34*, 14287–14301. [[CrossRef](#)]
74. Newton, R.; Holden, N.S.; Catley, M.C.; Oyelusi, W.; Leigh, R.; Proud, D.; Barnes, P.J. Repression of inflammatory gene expression in human pulmonary epithelial cells by small-molecule I kappa B kinase inhibitors. *J. Pharmacol. Exp. Ther.* **2007**, *321*, 734–742. [[CrossRef](#)] [[PubMed](#)]
75. Ten, R.M.; McKinstry, M.J.; Trushin, S.A.; Asin, S.; Paya, C.V. The signal transduction pathway of CD23 (Fc epsilon RIIB) targets I kappa B kinase. *J. Immunol.* **1999**, *163*, 3851–3857. [[CrossRef](#)] [[PubMed](#)]
76. Zhao, S.Y.; Qi, Y.; Liu, X.H.; Jiang, Q.B.; Liu, S.Y.; Jiang, Y.; Jiang, Z.F. Activation of NF-kappa B in bronchial epithelial cells from children with asthma. *Chin. Med. J.* **2001**, *114*, 909–911. [[PubMed](#)]

Disclaimer/Publisher's Note: The statements, opinions and data contained in all publications are solely those of the individual author(s) and contributor(s) and not of MDPI and/or the editor(s). MDPI and/or the editor(s) disclaim responsibility for any injury to people or property resulting from any ideas, methods, instructions or products referred to in the content.